Ranaghan, K., Mulholland, A., Harvey, J., Manby, F., Scrutton, N., Senthilkumar, K., Morris, W., Johannissen, L., & Masgrau, L. (2017). Ab Initio QM/MM Modeling of the Rate-Limiting Proton Transfer Step in the Deamination of Tryptamine by Aromatic Amine Dehydrogenase. *Journal of Physical Chemistry B*, *121*(42), 9785–9798. https://doi.org/10.1021/acs.jpcb.7b06892

Supporting Information

Ab Initio QM/MM Modelling of the Rate-Limiting Proton Transfer Step in the Deamination of Tryptamine by Aromatic Amine Dehydrogenase

Kara E. Ranaghan[a], William G. Morris[a], Laura Masgrau[b,c], Kittusamy Senthilkumar[d], Linus O. Johannissen[e], Nigel S. Scrutton[e], Jeremy N. Harvey[f], Frederick R. Manby[a] and Adrian J. Mulholland[a]*

[a]*Centre for Computational Chemistry, School of Chemistry, University of Bristol, Cantock's Close, Bristol, BS8 1TS, UK.*

[b]*Institut de Biotecnologia i de Biomedicina (IBB), Universitat Autònoma de Barcelona, 08193 Bellaterra (Barcelona), Spain*

[c]*Departament de Bioquímica i Biologia Molecular, Universitat Autònoma de Barcelona, 08193 Bellaterra (Barcelona), Spain*

[d]*Department of Physics, Bharathiar University, Coimbatore, India.*

[e]*Manchester Institute of Biotechnology, University of Manchester, Manchester, UK.*

[f]*Department of Chemistry, KU Leuven, Celestijnenlaan 200F, B-3001 Heverlee, Belgium.*

**Corresponding author: Prof. Adrian Mulholland (Adrian.Mulholland@bristol.ac.uk)*

Contents

1. MM MD simulations of AADH

A model of AADH with tryptamine was built using the crystal structure 2AGY.[1] Hydrogens were added to the system in accordance with pK_a predictions made by PROPKA[2] and the system was solvated in a cubic box of CHARMM TIP3P water molecules[3] using the solvate plugin in VMD.[4] The model comprised ~113,000 atoms. Parameters were assigned based on the CHARMM27 forcefield. All simulations were carried out using NAMD,[5] running on 64 processors. The positions of the hydrogen atoms were minimised for 5000 steps using the conjugate gradients (CG) algorithm keeping heavy atoms fixed. The positions of the water molecules were then minimised using 6000 steps of CG minimisation, keeping the protein fixed. The water molecules were then heated to 300 K over a period of 2.5 ps and then allowed to move for a further 5 ps in an NVT ensemble. The energy of system was then minimised for 10000 steps of CG minimisation. All atoms were then heated to 300 K over 5 ps and then allowed to equilibrate for 180 ps at constant temperature and pressure. The Nose-Hoover piston[6] and Langevin temperature control[7] were used during equilibration. The production simulations were then run for 100 ns using a time step of 2 fs and constraining the positions of hydrogen atoms using the SHAKE algorithm. Three replicate simulations were performed starting from separate heating phases with different initial velocities.

2. Activation entropy

The entropic contribution to the free energy is also important. A rough estimation of the entropic contribution to the barrier can be obtained by comparing the potential energy barrier calculated by adiabatic mapping with the classical free energy barrier resulting from umbrella sampling simulations.[8] However, in practice these calculations can be hard to converge, as is the case for AADH. From our previous work at the PM3-SRP/CHARMM level[9], $\Delta^{\ddagger}V$ is 19.2 kcal/mol for proton transfer to O2 of D128β and 14.6 kcal/mol for O1. $\Delta^{\ddagger}G$ is 12.5 kcal/mol for proton transfer to O2 of D128β and 16.4 kcal/mol for O1. The resulting entropic correction of 6.7 kcal/mol for proton transfer to O2 of D128β is much bigger than the −1.8 kcal/mol O1 at the PM3-SRP/CHARMM level. The activation entropy should be similar for both pathways, but to use an average value (2.5±6.0 kcal/mol) would not be meaningful due to the large standard

deviation. There is some structural rearrangement involved in the early part of the free energy profile for proton transfer to O2[9], but the entropic contribution should be similar for the two pathways. The error in the estimation of the $T\Delta S$ term is too high (±6 kcal/mol) to be meaningful here. Activation entropy terms (at 300 K) have been calculated for other enzymes e.g. 0.4 kcal/mol for para-hydroxybenzoate hydroxylase (PHBH)[8], 2.5 kcal/mol for chorismate mutase[8] and values between −4.2 and 2.7 kcal/mol for different steps of the reaction in cytidine deaminase10, showing that the activation entropy term is small, but of the same order of magnitude as the tunnelling contribution

Table S1: Average interatomic distances (in Å) from 3 100 ns simulations of AADH at 300 K using the CHARMM22 forcefield. Data from the first 10 ns is considered equilibration and is not included in the values presented here.

	SIM 1		SIM 2		SIM 3	
	AVE	**STDEV**	**AVE**	**STDEV**	**AVE**	**STDEV**
C1-O2	3.43	0.23	3.39	0.17	3.36	0.16
C1-O1	3.01	0.13	3.11	0.18	3.01	0.11
O2-H1	2.69	0.32	2.50	0.18	2.53	0.19
O1-H1	2.50	0.18	2.65	0.23	2.47	0.16
HE1-O7	2.82	0.11	2.83	0.11	2.82	0.11
HE1-A82O	1.96	0.16	2.00	0.18	2.02	0.20
HNT-O7	2.41	0.12	2.41	0.12	2.41	0.12
HNT-D84O	2.28	0.31	2.22	0.26	2.29	0.34
O7-D84 HN	2.14	0.22	2.01	0.17	2.12	0.22
O2-T172 HG1	1.91	0.20	1.86	0.17	1.83	0.16
O1-W160 HN	1.98	0.18	2.46	0.38	1.91	0.15

Table S2: Reaction energetics (in kcal/mol, relative to the reactant) and reaction coordinate values (**Z/Å**) from adiabatic mapping (E_{AM}) and CINEB (E_{CINEB}) calculations for proton transfer to O2 and O1 of D128β at the B3LYP/6-31G(d)/MM level of theory.

		O2				O1			
		Z	**E_{AM}**	**Z**	**E_{CINEB}**	**Z**	**E_{AM}**	**Z**	**E_{CINEB}**
PATH 1	**R**	-0.89	0.00	-0.89	0.00	-0.72	0.00	-0.72	0.00
	TS	0.1	11.58	0.18	11.56	0.20	7.78	0.15	7.75
	P	1.08	4.85	1.08	4.85	0.94	2.17	0.94	2.17
PATH 2	**R**	-0.84	0.00	-0.84	0.00	-0.77	0.00	-0.77	0.00
	TS	0.2	10.96	0.19	10.88	0.10	7.58	0.16	7.56
	P	1.00	4.41	1.00	4.41	0.99	1.84	0.99	1.84
PATH 3	**R**	-0.84	0.00	-0.84	0.00	-0.74	0.00	-0.74	0.00
	TS	0.2	10.19	0.19	10.16	0.20	9.39	0.17	9.29
	P	1.00	3.66	1.00	3.66	1.01	2.69	1.01	2.69
PATH 4	**R**	-0.81	0.00	-0.81	0.00	-0.70	0.00	-0.70	0.00
	TS	0.2	9.96	0.18	9.88	0.20	7.83	0.13	7.71
	P	1.01	5.39	1.01	5.39	0.94	2.38	0.94	2.38
PATH 5	**R**	-0.74	0.00	-0.74	0.00	-0.77	0.00	-0.77	0.00
	TS	0.30	9.99	0.23	9.82	0.10	8.04	0.11	7.98
	P	1.00	6.04	1.00	6.04	0.94	1.51	0.94	1.51
AVE	**R**	-0.82	0.00	-0.82	0.00	-0.74	0.00	-0.74	0.00
	TS	0.20	10.54 (±0.71)	0.19	10.46 (±0.75)	0.16	8.13 (±0.73)	0.14	8.06 (±0.70)
	P	1.02	4.87 (±0.91)	1.02	4.87 (±0.91)	0.96	2.12 (±0.46)	0.96	2.12 (±0.46)

Table S3: Average interatomic distances and hydrogen bonds with residues in the active site along the reaction paths for proton transfer to either O2 or O1 of D128β (B3LYP/6-31G(d)/MM). Distances are given in Å, upper number is the average and the number in parentheses is the standard deviation. See Figure 1 for atom labels.

	Proton transfer to O2 of D128				Proton transfer to O1 of D128		
	R	**TS**	**P**		**R**	**TS**	**P**
C1-H1	1.11 (0.00)	1.42 (0.01)	2.02 (0.03)	**C1-H1**	1.11 (0.00)	1.39 (0.02)	1.96 (0.03)
O2-C1	2.99 (0.04)	2.65 (0.01)	3.00 (0.03)	**O1-C1**	2.88 (0.02)	2.60 (0.01)	2.93 (0.03)
O2-H1	1.93 (0.05)	1.23 (0.01)	1.00 (0.00)	**O1-H1**	1.85 (0.03)	1.24 (0.01)	1.00 (0.00)
HE1-O7	2.79 (0.01)	2.78 (0.01)	2.77 (0.01)	**HE1-O7**	2.79 (0.02)	2.78 (0.02)	2.76 (0.02)
HE1-A82 O	1.77 (0.02)	1.79 (0.03)	1.80 (0.03)	**HE1-A82 O**	1.76 (0.03)	1.78 (0.03)	1.80 (0.04)
HNT-O7	2.19 (0.02)	2.19 (0.02)	2.14 (0.03)	**HNT-O7**	2.27 (0.02)	2.27 (0.03)	2.21 (0.03)
HNT-D84 O	2.03 (0.07)	2.13 (0.07)	2.14 (0.08)	**HNT-D84 O**	2.13 (0.17)	2.26 (0.20)	2.26 (0.21)
O7-D84 HN	2.00 (0.06)	2.01 (0.06)	2.00 (0.06)	**O7-D84 HN**	1.96 (0.08)	1.96 (0.08)	1.93 (0.08)
O2-T172 HG1	1.78 (0.02)	1.88 (0.03)	1.92 (0.02)	**O2-T172 HG1**	1.81 (0.02)	1.80 (0.01)	1.88 (0.01)
O1-W160 HN	1.96 (0.06)	2.02 (0.06)	2.13 (0.06)	**O1-W160 HN**	1.92 (0.07)	2.19 (0.16)	2.31 (0.14)

Table S4: Average contribution (in kcal/mol) of T172β and W160β to the QM/MM electrostatic energy (QM/MM_{el}) at different points along the reaction pathway for proton transfer to O2 or O1 of D128β (B3LYP/6-31G(d)/MM). The standard deviation of the average energy is given in parentheses.

	Proton transfer to O2 of D128 β		**Proton transfer to O1 of D128 β**	
	QM/MM_{el} T172β	**QM/MM_{el} W160β**	**QM/MM_{el} T172β**	**QM/MM_{el} W160β**
R	-15.96 (±2.85)	-17.22 (±2.63)	-15.68 (±0.57)	-16.73 (±0.67)
TS	-6.73 (±3.74)	-9.30 (±4.33)	-9.03 (±0.34)	-12.44 (±0.40)
P	-5.92 (±1.75)	-7.53 (±1.10)	-5.36 (±0.33)	-6.55 (±0.49)

Table S5: Average potential energy barriers ($\Delta^{\ddagger}V$) (relative to the reactant) and reaction energies ($\Delta_r V$) calculated with DFT/6-31G(d), DFT/6-311+G(d), (L)MP2/(aug)-cc-pVTZ, SCS-(L)MP2/(aug)-cc-pVTZ and LCCSD(T)/(aug)-cc-pVTZ QM/MM methods on B3LYP/6-31G(d)/MM and BH&HLYP/6-31G(d)/MM optimized geometries, and corrected for zero point energy (ZPE) effects. All reaction coordinate values are in Å and energies are in kcal/mol. The L in these acronyms indicates that local approximations were used for the ab initio methods and (aug) indicates that only the basis functions for oxygen atoms were augmented.

		Z	DFT	DFT Larger basis	MP2	LMP2	SCS-MP2	SCS-LMP2	LCCSD(T)
$\Delta^{\ddagger}V_{O2}$	**B3LYP**	0.19	7.71	11.61	6.92	11.99	6.84	11.87	13.93
	BH&HLYP	0.19	10.51	14.34	7.40	12.10	7.51	12.16	13.65
$\Delta_r V_{O2}$	**B3LYP**	0.14	4.58	7.66	-0.38	4.64	-0.15	4.88	6.04
	BH&HLYP	0.16	2.83	5.52	-1.08	3.64	-0.61	4.11	3.70
$\Delta^{\ddagger}V_{O1}$	**B3LYP**	1.02	5.07	8.98	4.65	9.28	4.12	8.72	11.23
	BH&HLYP	1.10	7.30	11.24	4.80	9.31	4.58	9.06	10.69
$\Delta_r V_{O1}$	**B3LYP**	0.96	1.77	5.43	-4.24	0.80	-4.73	0.35	2.10
	BH&HLYP	1.00	1.33	4.75	-3.29	1.71	-2.99	2.02	2.21

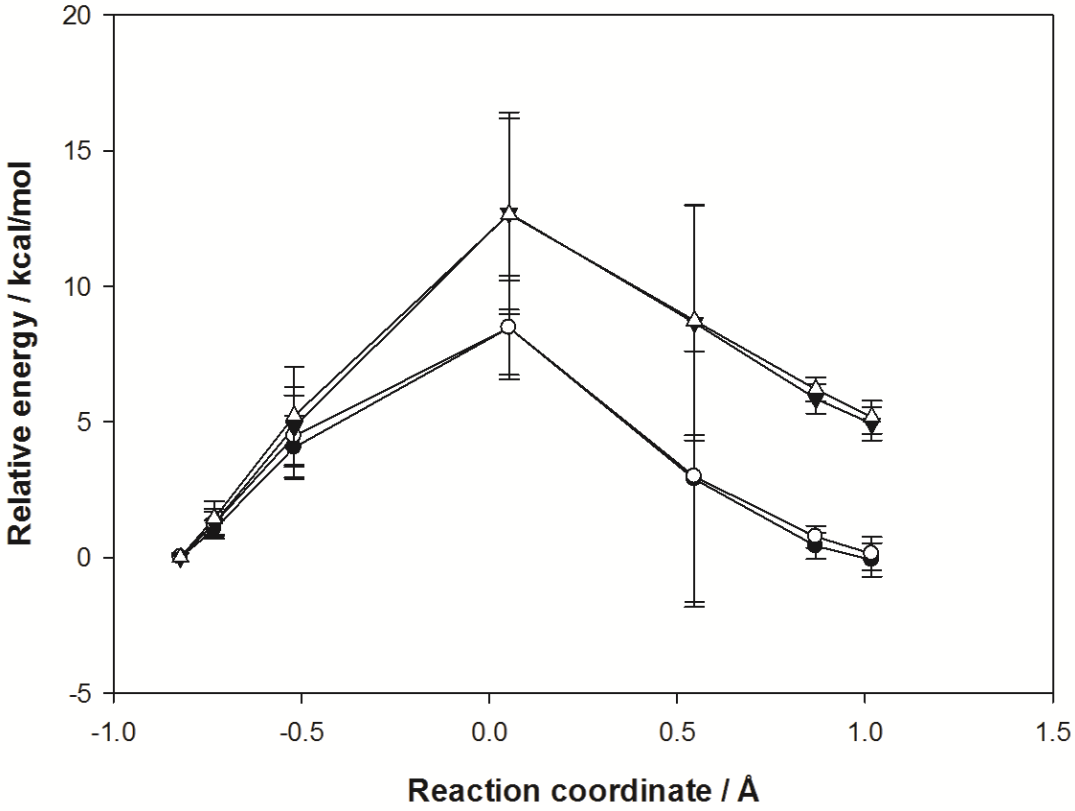

Figure S1: Comparison of the average reaction profiles (relative to the reactant) for proton transfer to O2 of D128β calculated with MP2 (using the B3LYP/6-31G(d)/MM CINEB geometries) with and without local approximations. Black circles: MP2/(aug)-cc-pVTZ/MM; white circles: LMP2/(aug)-cc-pVTZ/MM; black triangles: SCS-MP2/(aug)-cc-pVTZ/MM; white triangles: SCS-LMP2/(aug)-cc-pVTZ/MM. Energies are plotted as a function of reaction coordinate for comparison, no reaction coordinate was used in the generation of the profiles. Error bars indicate the standard deviation of the average energy.

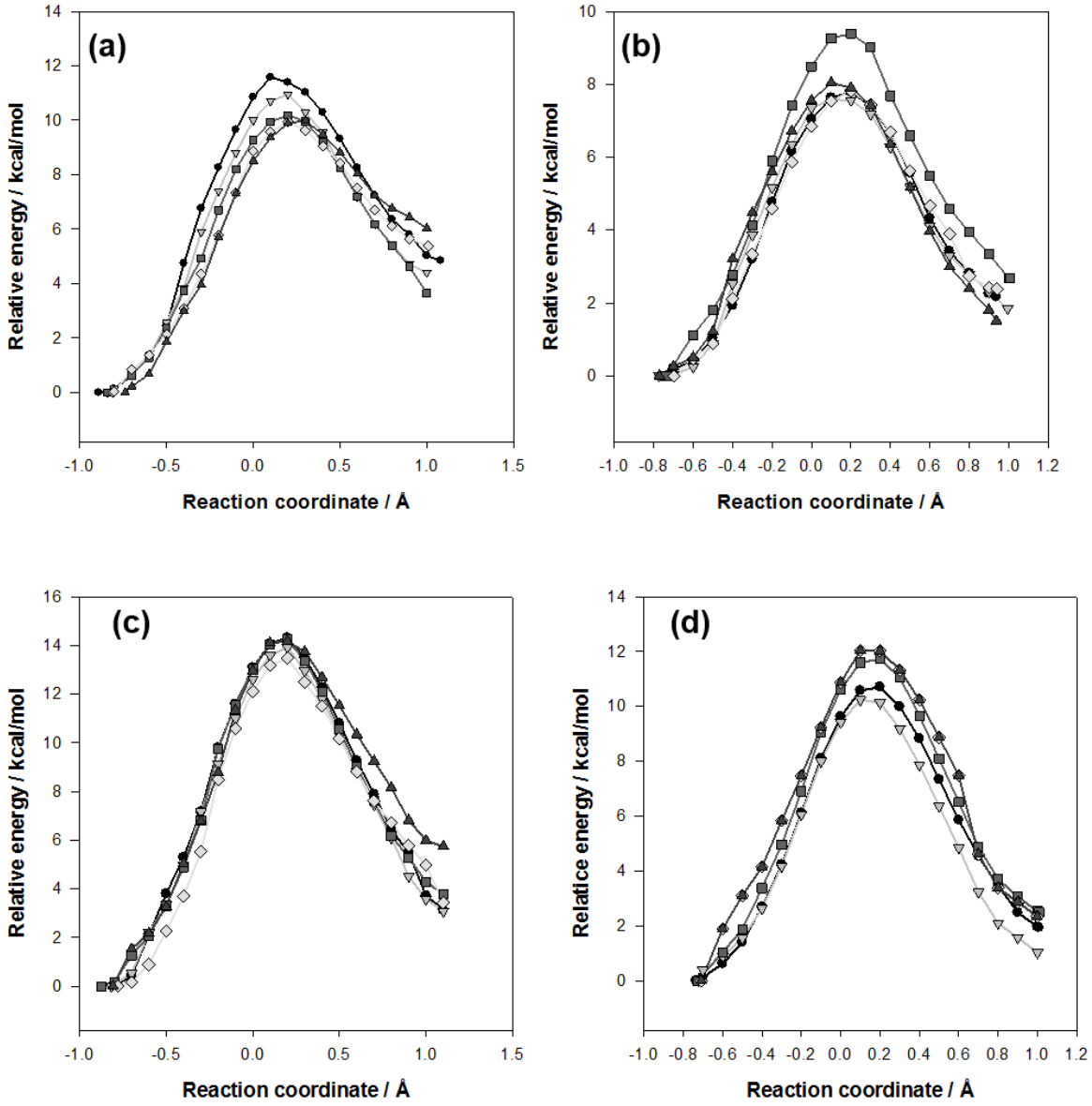

Figure S2: Potential energy profiles (relative to the reactant) for proton transfer to the two carboxylate oxygens of D128β generated by adiabatic mapping along a defined reaction coordinate. (a) Proton transfer to O2 of D128β calculated using the B3LYP/6-31G(d)/MM method; (b) Proton transfer to O1 of D128β calculated using the B3LYP/6-31G(d)/MM method; (c) Proton transfer to O2 of D128β calculated using the BH&HLYP/6-31G(d)/MM method; (d) Proton transfer to O1 of D128β calculated using the BH&HLYP/6-31G(d)/MM method.

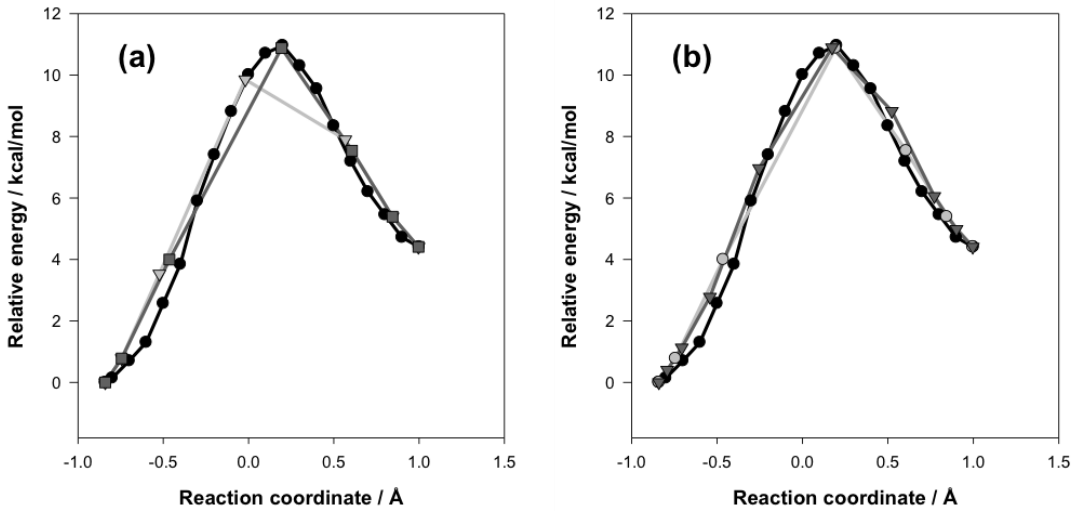

Figure S3 (a) NEB and climbing image NEB profiles compared to adiabatic mapping (black circles, adiabatic mapping profile; grey triangles, NEB profile optimized with 7 images; grey squares, CINEB profile from 7 starting images). (b) CINEB profiles optimized with 7 and 10 initial images compared to the adiabatic mapping profile (black circles, adiabatic mapping; grey circles, CINEB profile from 7 initial images; and grey triangles, CINEB profile from 10 initial images). No reaction coordinate is defined in the NEB and CINEB optimizations; the data is plotted relative to the energy of the reactant and against the reaction coordinate to aid the comparison with the adiabatic mapping profile. All profiles are calculated at the B3LYP/6-31G(d)/MM level of theory and correspond to PATH2 of proton transfer to O2.

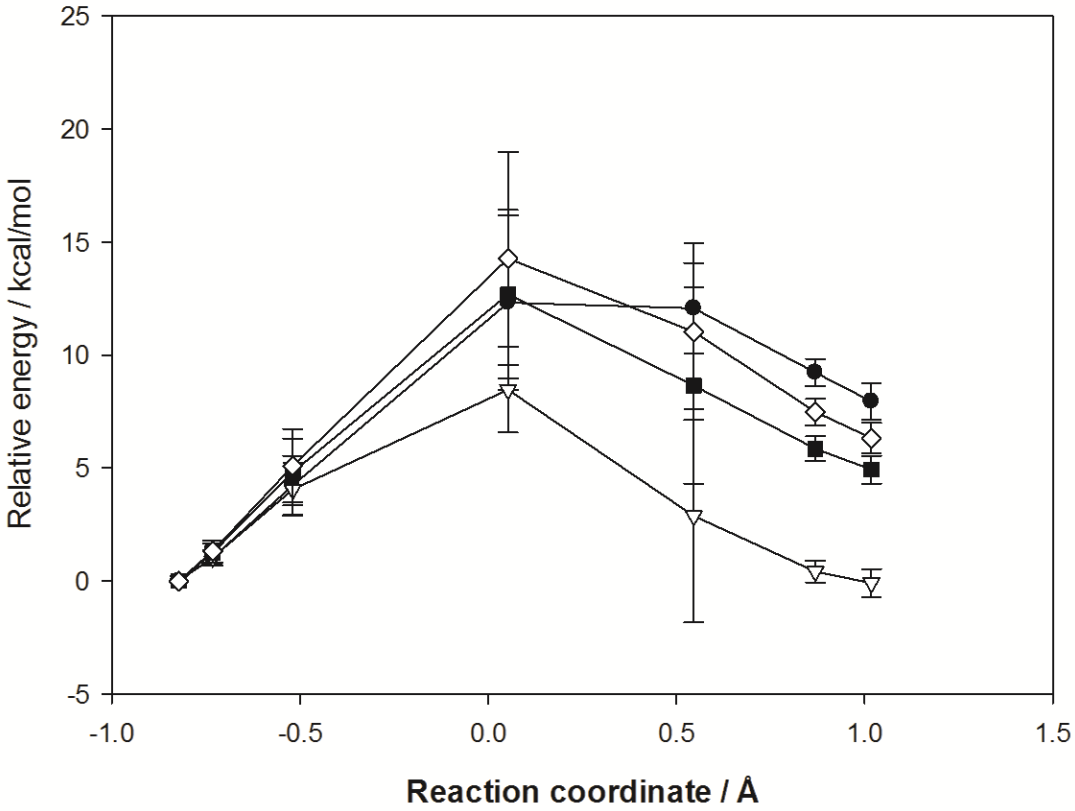

Figure S4: Comparison of the average reaction profiles (relative to the reactant) calculated for proton transfer to O2 of D128β at the B3LYP/6-311+G(d)/MM (black circle), MP2/(aug)-cc-pVTZ/MM (white triangle), SCS-MP2/(aug)-cc-pVTZ/MM (black square) and LCCSD(T)/(aug)-cc-pVTZ/MM (white diamond) levels of theory (using the B3LYP/6-31G(d)/MM CINEB geometries). Energies are plotted as a function of reaction coordinate for comparison, no reaction coordinate was used in the generation of the profiles. Error bars indicate the standard deviation of the average energy.

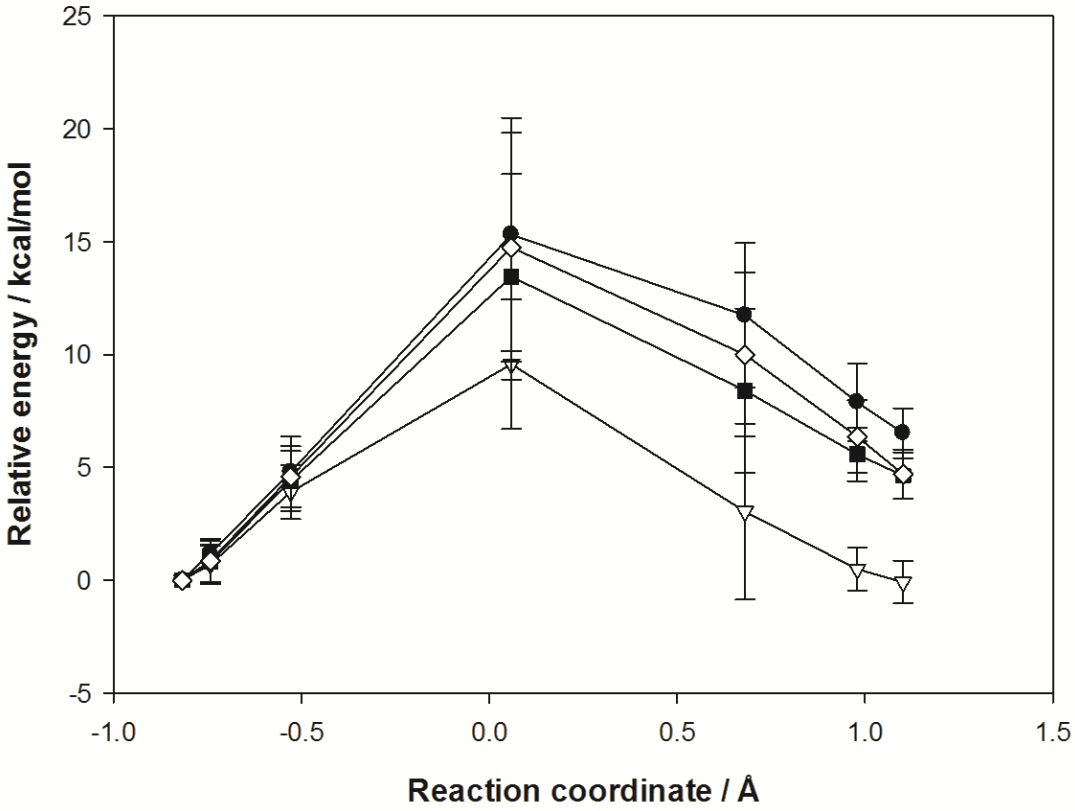

Figure S5: Comparison of the average reaction profiles (relative to the reactant) calculated for proton transfer to O2 of D128β at the BH&HLYP/6-311+G(d)/MM (black circle), MP2/(aug)-cc-pVTZ/MM (white triangle), SCS-MP2/(aug)-cc-pVTZ/MM (black square) and LCCSD(T)/(aug)-cc-pVTZ /MM (white diamond) levels of theory (using the BH&HLYP/6-31G(d)/MM CINEB geometries). Energies are plotted as a function of reaction coordinate for comparison, no reaction coordinate was used in the generation of the profiles. Error bars indicate the standard deviation of the average energy.

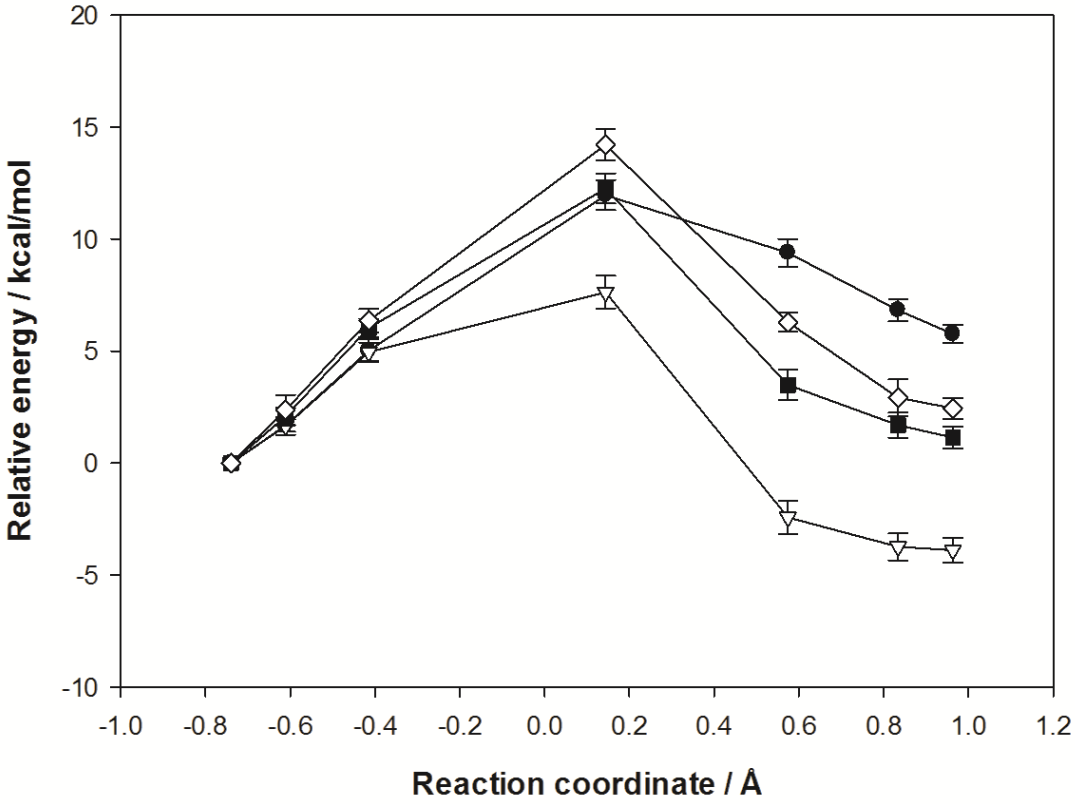

Figure S6: Comparison of the average reaction profiles (relative to the reactant) calculated for proton transfer to O1 of D128β at the B3LYP/6-311+G(d)/MM (black circle), MP2/(aug)-cc-pVTZ/MM (white triangle), SCS-MP2/(aug)-cc-pVTZ/MM (black square) and LCCSD(T)/(aug)-cc-pVTZ /MM (white diamond) levels of theory (using the B3LYP/6-31G(d)/MM CINEB geometries). Energies are plotted as a function of reaction coordinate for comparison, no reaction coordinate was used in the generation of the profiles. Error bars indicate the standard deviation of the average energy.

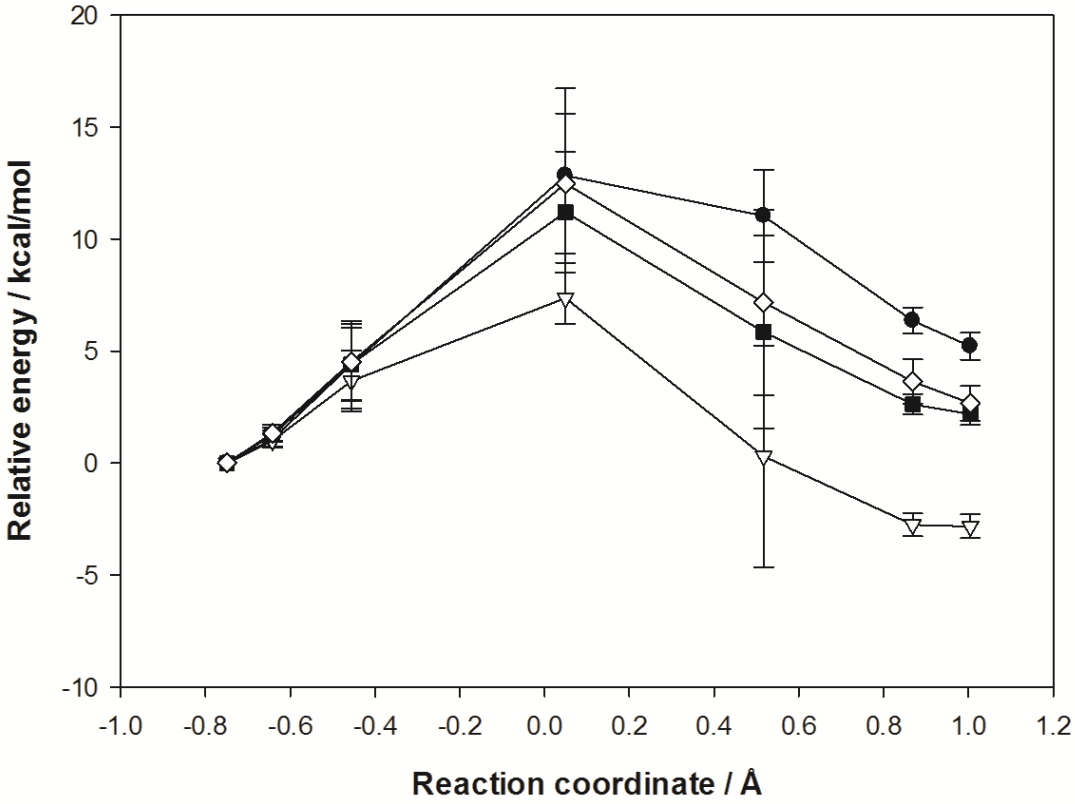

Figure S7: Comparison of the average reaction profiles (relative to the reactant) calculated for proton transfer to O1 of D128β at the BH&HLYP/6-311+G(d)/MM (black circle), MP2/(aug)-cc-pVTZ/MM (white triangle), SCS-MP2/(aug)-cc-pVTZ/MM (black square) and LCCSD(T)/(aug)-cc-pVTZ/MM (white diamond) levels of theory (using the BH&HLYP/6-31G(d)/MM CINEB geometries). Energies are plotted as a function of reaction coordinate for comparison, no reaction coordinate was used in the generation of the profiles. Error bars indicate the standard deviation of the average energy.

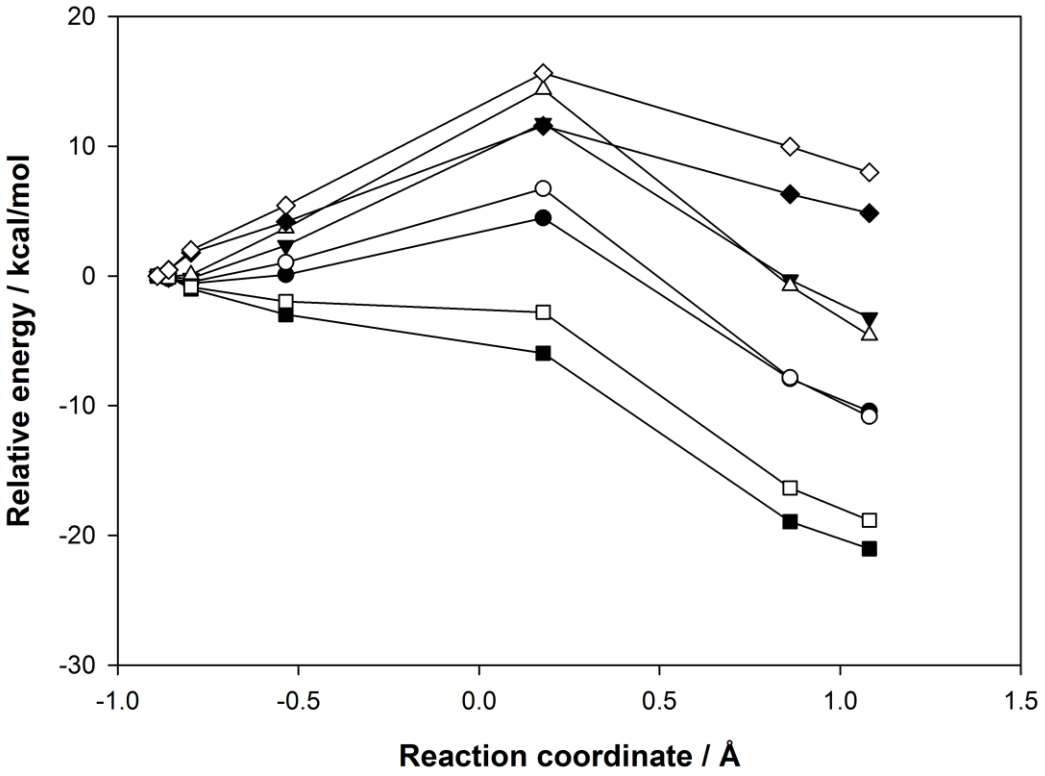

Figure S8: Comparison a representative potential energy profile for proton abstraction by O2 of D128β in the enzyme, gasphase and solution using solvent continuum models calculated with B3LYP as the QM method. The gasphase and solution energies are single point energy calculations on structures obtained from optimization within the enzyme without further optimization as the idea is to compare the effect of the environment not any differences in reaction pathway in different media. Black squares: B3LYP/6-31G(d) gasphase; white squares B3LYP/6-311+G(d) gasphase; black circles B3LYP/6-31G(d)/PCM; white circles B3LYP/6-311+G(d)/PCM; black triangles B3LYP/6-31G(d)/SM8; white triangles B3LYP/6-311+G(d)/SM8, black diamonds B3LYP/6-31G(d)/CHARMM27; white diamonds B3LYP/6-311+G(d)/CHARMM27. Energies are relative to the reactant and plotted as a function of reaction coordinate for comparison, no reaction coordinate was used in the generation of the profiles.

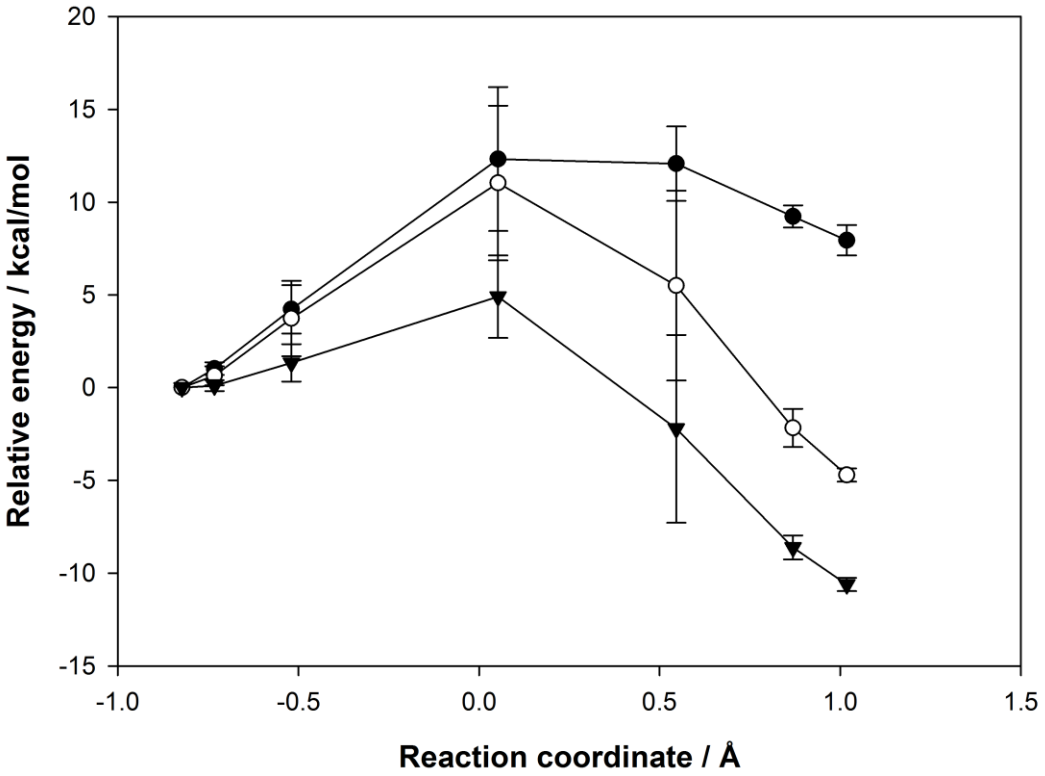

Figure S9: Comparison of the average reaction profile for proton abstraction by O2 of D128β in the enzyme (black circles) (B3LYP/6-311+G(d)//B3LYP/6-31G(d)/MM) and in solution using the SM8 (white circles) and PCM (black triangles) solvent continuum models at the B3LYP/6-311+G(d) level of theory. Energies are relative to the reactant and plotted as a function of reaction coordinate for comparison, no reaction coordinate was used in the generation of the profiles. Error bars indicate the standard deviation of the average energy.

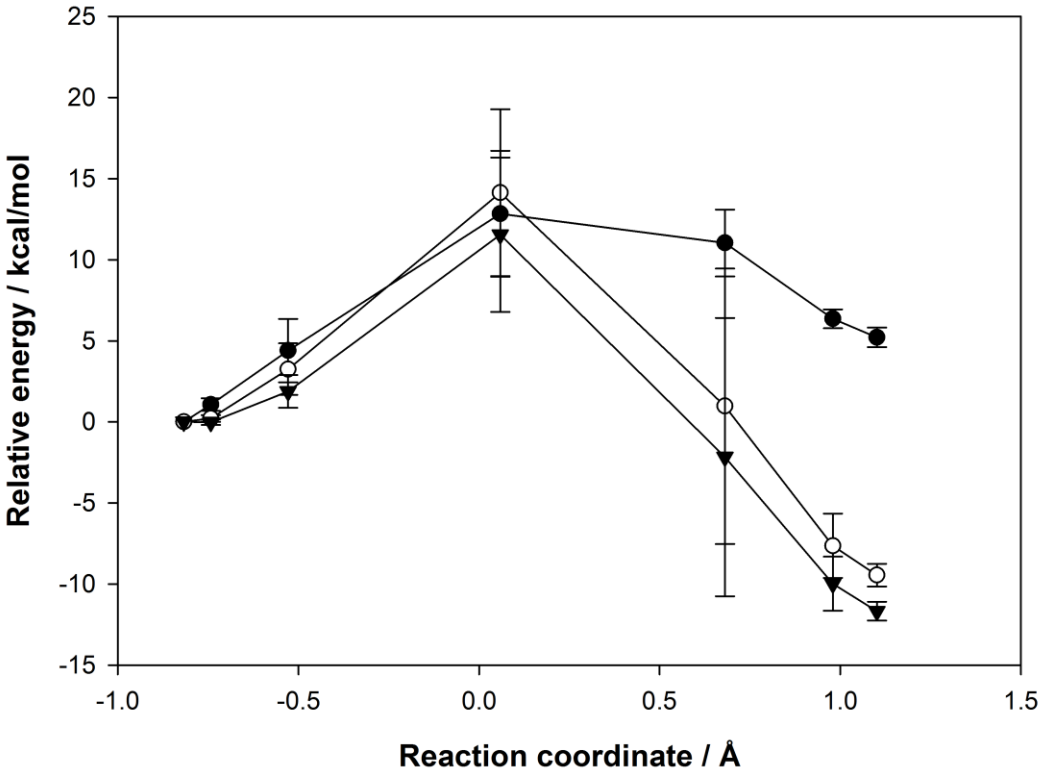

Figure S10: Comparison of the average reaction profile for proton abstraction by O2 of D128 β in the enzyme (black circles) (BH&HLYP/6-311+G(d)//BH&HLYP/6-31G(d)/MM) and in solution using the SM8 (white circles) and PCM (black triangles) solvent continuum models at the BH&HLYP/6-311+G(d) level of theory. Energies are relative to the reactant and plotted as a function of reaction coordinate for comparison, no reaction coordinate was used in the generation of the profiles. Error bars indicate the standard deviation of the average energy.

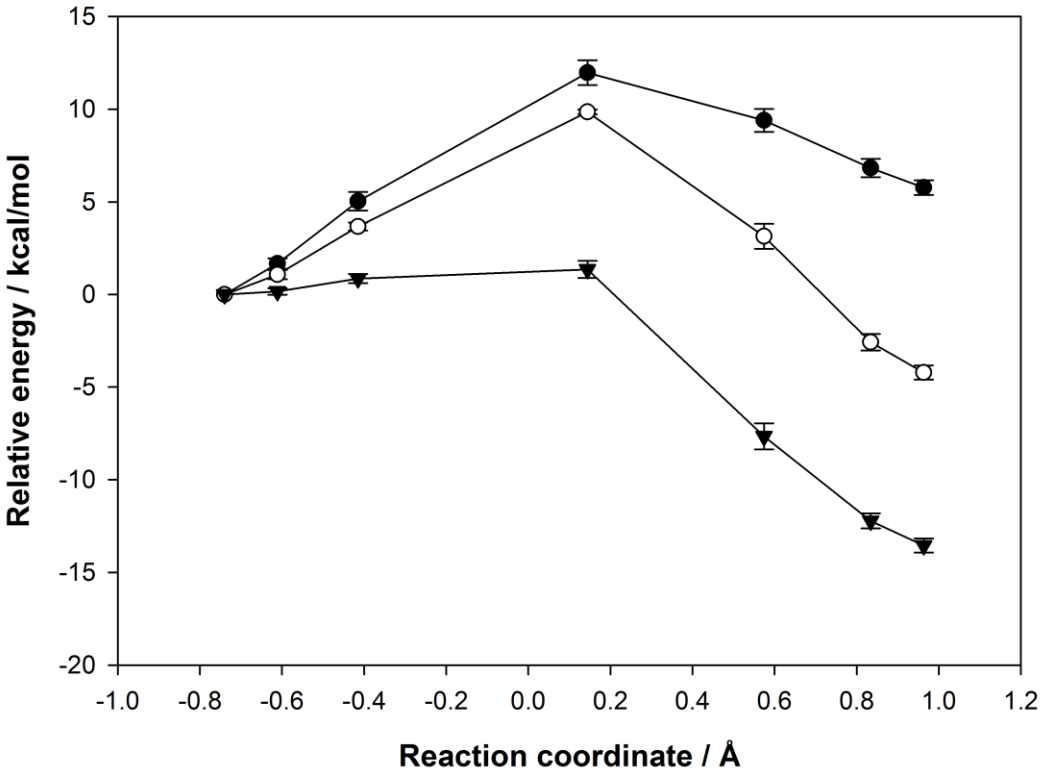

Figure S11: Comparison of the average reaction profile for proton abstraction by O1 of D128β in the enzyme (black circles) (B3LYP/6-311+G(d)//B3LYP/6-31G(d)/MM) and in solution using the SM8 (white circles) and PCM (black triangles) solvent continuum models at the B3LYP/6-311+G(d) level of theory. Energies are relative to the reactant and plotted as a function of reaction coordinate for comparison, no reaction coordinate was used in the generation of the profiles. Error bars indicate the standard deviation of the average energy.

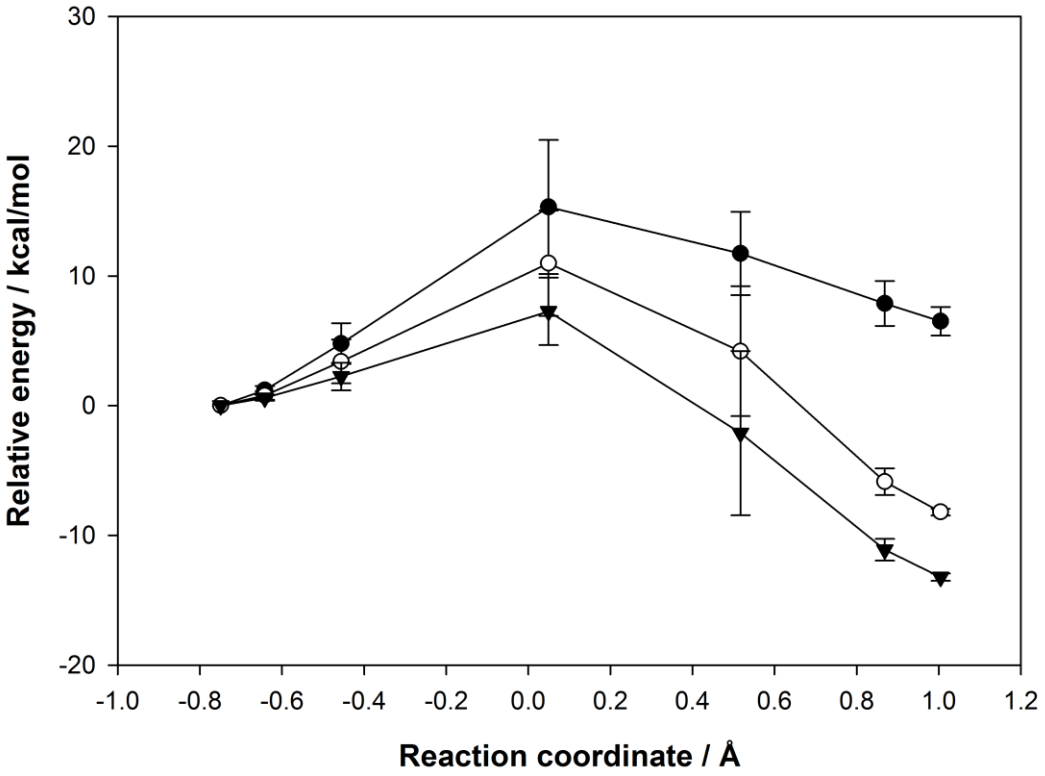

Figure S12: Comparison of the average reaction profile for proton abstraction by O1 of D128 β in the enzyme (black circles) (BH&HLYP/6-311+G(d)//BH&HLYP/6-31G(d)/MM) and in solution using the SM8 (white circles) and PCM (black triangles) solvent continuum models at the BH&HLYP/6-311+G(d) level of theory. Energies are relative to the reactant and plotted as a function of reaction coordinate for comparison, no reaction coordinate was used in the generation of the profiles.

3. References

1. Masgrau, L.; Roujeinikova, A.; Johannissen, L.; Hothi, P.; Basran, J.; Ranaghan, K.; Mulholland, A.; Sutcliffe, M.; Scrutton, N.; Leys, D. Atomic Description of an Enzyme Reaction Dominated by Proton Tunneling. *Science* **2006,** *312*, 237-241.

2. Olsson, M. H. M.; Sondergaard, C. R.; Rostkowski, M.; Jensen, J. H. PROPKA3: Consistent Treatment of Internal and Surface Residues in Empirical pK(a) Predictions. *J. Chem. Theory Comput.* **2011,** *7*, 525-537.

3. Jorgensen, W. L.; Chandrasekhar, J.; Madura, J. D.; Impey, R. W.; Klein, M. L. Comparison of Simple Potential Functions for Simulating Liquid Water. *J. Chem. Phys.* **1983,** *79*, 926-935.

4. Humphrey, W.; Dalke, A.; Schulten, K. VMD: Visual Molecular Dynamics. *J. Mol. Graph.* **1996,** *14*, 33-38.

5. Phillips, J. C.; Braun, R.; Wang, W.; Gumbart, J.; Tajkhorshid, E.; Villa, E.; Chipot, C.; Skeel, R. D.; Kale, L.; Schulten, K. Scalable Molecular Dynamics with NAMD. *J. Comput. Chem.* **2005,** *26*, 1781-1802.

6. Martyna, G. J.; Tobias, D. J.; Klein, M. L. Constant-Pressure Molecular-Dynamics Algorithms. *J. Chem. Phys.* **1994,** *101*, 4177-4189.

7. Feller, S. E.; Zhang, Y. H.; Pastor, R. W.; Brooks, B. R. Constant-Pressure Molecular-Dynamics Simulation - The Langevin Piston Method. *J. Chem. Phys.* **1995,** *103*, 4613-4621.

8. Claeyssens, F.; Harvey, J. N.; Manby, F. R.; Mata, R. A.; Mulholland, A. J.; Ranaghan, K. E.; Schuetz, M.; Thiel, S.; Thiel, W.; Werner, H.-J. High-Accuracy

Computation of Reaction Barriers in Enzymes. *Angew. Chem. Int. Edit.* **2006,** *45*, 6856-6859.

9. Masgrau, L.; Ranaghan, K. E.; Scrutton, N. S.; Mulholland, A. J.; Sutcliffe, M. J. Tunneling and Classical Paths for Proton Transfer in an Enzyme Reaction Dominated by Tunneling: Oxidation of Tryptamine by Aromatic Amine Dehydrogenase. *J. Phys. Chem. B* **2007,** *111*, 3032-3047.

10. Kazemi, M.; Himo, F.; Aqvist, J. Enzyme Catalysis by Entropy Without Circe Effect. *Proc. Nat. Acad. Sci. USA* **2016,** *113*, 2406-2411.